Node-like excitations in superconducting $PbMo_6S_8$ probed by scanning tunneling spectroscopy

C. Dubois,* A. P. Petrovic, G. Santi, C. Berthod, A. A. Manuel, M. Decroux, and Ø. Fischer
DPMC-MaNEP, Université de Genève, Quai Ernest-Ansermet 24, 1211 Genève 4, Switzerland

M. Potel and R. Chevrel
Sciences Chimiques de Rennes, CSM UMR CNRS 6226, Université de Rennes 1, Avenue du Général Leclerc, 35042 Rennes Cedex, France

(Received 22 December 2006; published 5 March 2007)

We present a scanning tunneling spectroscopy study on the Chevrel phase $PbMo_6S_8$, an extreme type-II superconductor with a coherence length only slightly larger than in high-T_c cuprates. Tunneling spectra measured on atomically flat terraces are spatially homogeneous and show well-defined coherence peaks. The low-energy spectral weight, the zero bias conductance, and the temperature dependence of the gap are incompatible with a conventional isotropic *s*-wave interpretation, revealing the presence of low-energy excitations in the superconducting state. We show that our data are consistent with the presence of nodes in the superconducting gap.

DOI: 10.1103/PhysRevB.75.104501 PACS number(s): 74.70.Dd, 68.37.Ef, 74.20.Rp

The Chevrel phase family of superconductors attracted great attention in the 1970s and 1980s since several of its members possessed unprecedentedly high upper critical fields, while others displayed astonishing properties resulting from the coexistence of superconductivity and magnetism.[1] Interest in these compounds faded somewhat with the advent of high-temperature superconductors (HTSs). However, in the quest to understand the pairing mechanism in HTSs, research has recently diversified into other strongly correlated electron systems which exhibit unusual superconductivity. For instance, heavy fermions,[2,3] borocarbides,[4,5] organics,[6,7] and ruthenates[8,9] have already provided vital insight into the fundamental questions of gap symmetry and the interplay between superconductivity and magnetism. In this context, the properties of the Chevrel phases render them particularly relevant and interesting. Among these compounds, $PbMo_6S_8$ is one of the most remarkable, with its high critical temperature of 14 K and a strikingly high upper critical field of about 60 T, corresponding to a very short coherence length $\xi \approx 23$ Å (estimated from the critical field[10] using the Ginzburg-Landau theory). This value is comparable to those found in the HTSs (e.g., 11, 20, and 30 Å for $Bi_2Sr_2CaCu_2O_{8+\delta}$, $YBa_2C_3O_{7-\delta}$, $La_{2-x}Sr_xCuO_4$, respectively[11]). With a $\kappa = \lambda/\xi$ above 100, $PbMo_6S_8$ is clearly an extreme type-II superconductor.

Scanning tunneling spectroscopy (STS) today plays a central role in the study of superconductors at an atomic scale. In particular, STS investigations have revealed significant differences between classical BCS and high-temperature superconductors,[12] notably the very large gaps in the spectra consistent with *d*-wave symmetry and the spatial dependence of the electronic structure in the vortex cores, which differ radically from what is observed in conventional superconductors.[13,14] One possible contribution to these differences is the very small size of the Cooper pairs in HTSs, resulting in a deviation from mean-field theory. Compared with HTSs, $PbMo_6S_8$ is stoichiometric, its structure is three-dimensional (3D), and, unlike other Chevrel phases, it is not known to display competition between superconductivity and magnetism. We consider it to be a bridge between classical type-II superconductors and HTSs. When the Chevrel phases were first studied, it was assumed during most investigations that they were classical *s*-wave superconductors[1] similar to other type-II superconductors known at that time. However, the very small Cooper pair size raises questions over the microscopic nature of the superconducting state in $PbMo_6S_8$ and, more generally, the role of short coherence length in unconventional superconductivity.

In this paper, we present the STS study of $PbMo_6S_8$ single crystals. We show tunneling spectra measured on atomically flat cleaved surfaces at different temperatures. The central result reported here is that the spectra obtained reproducibly on different crystals are clearly incompatible with the classical *s*-wave model and reveal the presence of low-energy excitations between the superconducting coherence peaks.

The high-quality $PbMo_6S_8$ single crystals were prepared by both chemical-vapor transport in silica tubes and high-temperature melt techniques in sealed Mo crucibles.[15] They display a sharp superconducting transition at $T_c = 14$ K with width $\Delta T_c = 0.3$ K determined by ac susceptibility measurements. $PbMo_6S_8$ crystallizes in a "quasicubic" rhombohedral lattice, space group $R\bar{3}$,[1] with the threefold axis along the [111] direction. We obtained flat (001) surfaces by cleaving the crystals using a blade under an optical microscope. The STS measurements were carried out using a home-built scanning tunneling microscope, featuring an *XY* stage[16] to target the micrometer-sized crystals. We use electrochemically etched Ir tips and measure the differential conductivity using a standard lock-in technique.

The surface topography imaged at 1.8 K with the tip perpendicular to the (001) plane reveals large flat terraces separated by long parallel steps. Figure 1 shows a typical step of height of 5.9 ± 1.1 Å. This corresponds to the distance between the Pb planes, which are the natural cleavage planes of $PbMo_6S_8$. The surfaces investigated were atomically flat with an rms roughness under 0.7 Å.

Homogeneous spectra have been obtained at a large number of positions on different crystals along lines [Fig. 2(a)] and on maps extending over a range of several hundred ang-

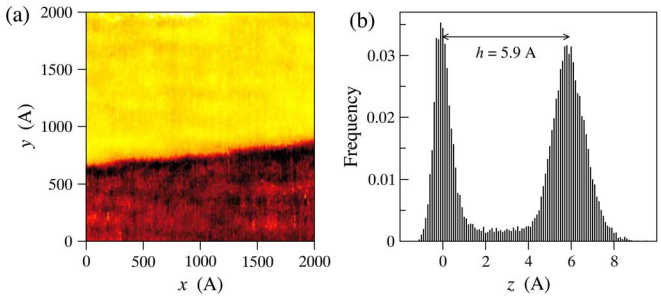

FIG. 1. (Color online) Topographic characterization. (a) Large-scale topography (T=1.8 K, R_t=50 MΩ). (b) Corresponding height histogram showing a unit step of height of 5.9±1.1 Å.

stroms. We have verified that the spectra obtained by varying the tunnel resistance R_t all collapse onto a single curve [Fig. 2(b)], which confirms true vacuum tunneling conditions. It is also important to mention that our measurements have always shown the same spectroscopic signature regardless of sample and cleavage. The spectra present well developed and homogeneous coherence peaks. The zero-bias conductance (ZBC) is homogeneous with a value of ~30% of the high-energy conductance [Fig. 2(c)]. This unusually large value, also reported by early planar-junction experiments,[17] could, in principle, be due to an extrinsic influence such as surface impurities. However, the high reproducibility of the ZBC leads us to believe that it is intrinsic to this material. Furthermore, we stress that $PbMo_6S_8$ does not suffer from surface contamination or aging effects.

The shape of the spectra reveals the presence of low-energy excitations which cannot be explained by thermal broadening and is reminiscent of that observed in HTSs (Fig. 3). We have therefore performed fits to our experimental spectra using single-band model and different singlet-gap symmetry scenarios. STS is a direct probe of the local quasiparticle density of states (DOS) and is therefore not sensitive to the phase of the order parameter. Hence, it cannot determine whether a sign change occurs, but it can reveal the presence of regions where the gap function is zero (nodes) or nearly zero (node-like). Using the BCS Green's function and including lifetime effects due to impurity scattering, the quasiparticle DOS reads

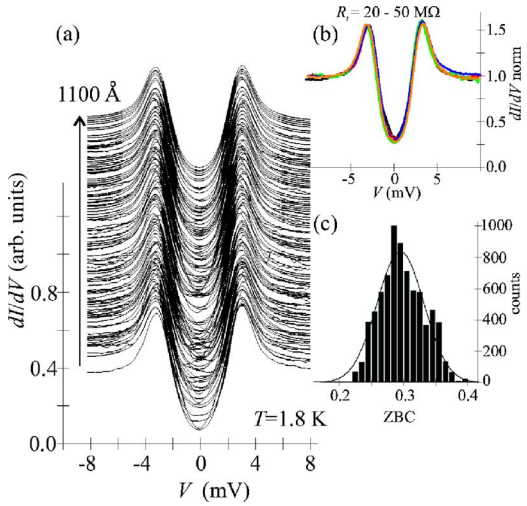

FIG. 2. (Color online) (a) Spectroscopic trace along a 1100 Å path with one spectrum every 8.8 Å. The spectra are offset for clarity (T=1.8 K, R_t=25 MΩ). (b) Normalized conductance spectra obtained at various R_t from 20 to 50 MΩ. (c) Histogram of the zero-bias conductance in ~7500 spectra normalized to the conductance at 8 mV. The standard deviation is 0.04.

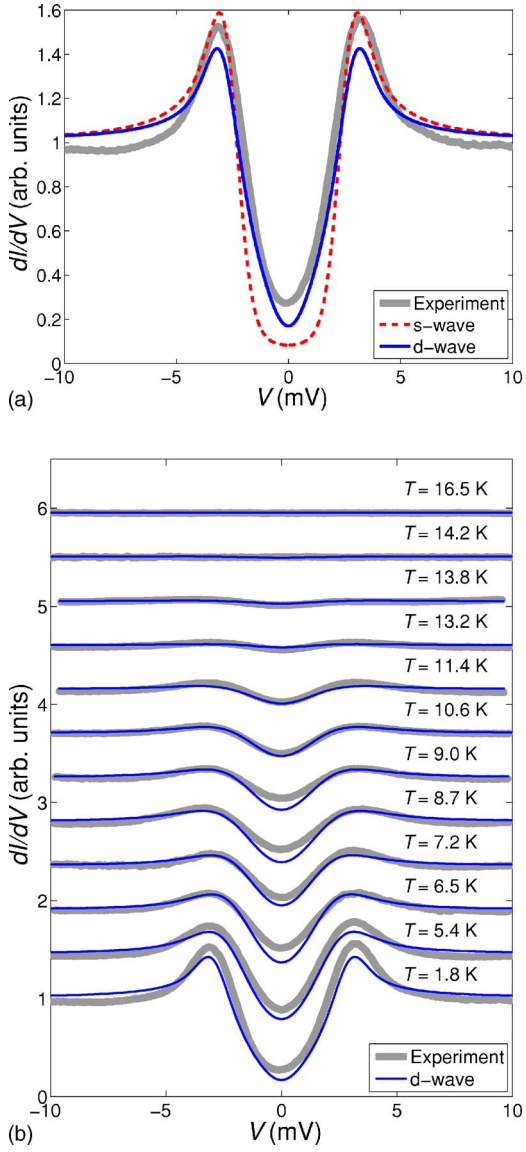

FIG. 3. (Color online) (a) Experimental dI/dV spectrum at 1.8 K (thick line) compared to the s- and d-wave fits described in the text (dashed and solid lines, respectively). (b) dI/dV spectra obtained at various temperatures (thick lines) and d-wave fits (thin lines). Each experimental spectrum is normalized so as to ensure state conservation within the measurement energy range and is offset by 0.45 with respect to the previous one for clarity.

$$N(\omega) = -\frac{1}{\pi}\sum_k \mathrm{Im}\left[\frac{\omega + \xi_k + i\Gamma}{(\omega + i\Gamma)^2 - \xi_k^2 - |\Delta_k|^2}\right], \qquad (1)$$

where $\xi_k = \epsilon_k - \epsilon_F$ are the band energies relative to the Fermi level, Δ_k the superconducting gap, and Γ the scattering rate.

TABLE I. Lowest-order representations compatible with rhombohedral symmetry for the gap $\Delta_{\boldsymbol{k}}=\Delta_0\psi(\boldsymbol{k})$. $\hat{z}$ is chosen along the three fold axis.

	Pairing symmetry[a]	$\boldsymbol{k}$ dependence of the gap, $\psi(\boldsymbol{k})$	Relation to point-group symmetry
$\mathcal{R}_1$	s	1	Preserving (isotropic)
$\mathcal{R}_2$	d	$(k_x \pm ik_y)^2$	Breaking
$\mathcal{R}_3$	d	$k_z(k_x \pm ik_y)$	
$\mathcal{R}_4$	d	$(k_x^2+k_y^2)$	Preserving
$\mathcal{R}_5$	d	$\frac{1}{2}(3k_z^2-1)$	

[a]Reference 18.

We have calculated the DOS, assuming a spherically symmetric Fermi surface; the relevance of the real band structure will be discussed below.

The gap representations compatible with the rhombohedral symmetry are very similar to those for the hexagonal group in Ref. 19. We shall focus on the lowest-order gaps (s and d), which are listed in Table I. Representations $\mathcal{R}_2$ and $\mathcal{R}_4$ give identical DOS as they only differ by a phase factor. Furthermore, representation $\mathcal{R}_3$, although behaving differently close to the nodes, gives a DOS which is indistinguishable from those of $\mathcal{R}_2$ and $\mathcal{R}_4$ once integrated over the Fermi surface. We thus group these three representations under the collective label "d wave."[18] In contrast, the typical DOS from the last d-wave representation $\mathcal{R}_5$ shows greatly reduced peaks (similar to higher-order g-wave cases not shown in Table I), which are totally incompatible with the observed spectra and will therefore not be further discussed here.

The average experimental spectrum at 1.8 K is shown in Fig. 3(a) together with the fits. The calculated spectra take into account the temperature smearing and a Gaussian broadening with a half-width at half maximum of 0.4 mV. This value corresponds to the lock-in amplitude and sets the maximum experimental resolution. The fits are defined to optimally reproduce the peak energy positions and widths. The isotropic s wave for $\Delta_0=2.6$ meV and $\Gamma=0.2$ meV clearly fails to describe the spectrum between the coherence peaks. In direct contrast, the d-wave cases for $\Delta_0=2.95$ meV and $\Gamma=0$ meV provide a much better fit in the low-energy region, which is the most sensitive to changes in the gap symmetry. Attempting to fit the ZBC with a s-wave symmetry by raising Γ or introducing a normal residual DOS (Ref. 20) fails due to either a dramatic coherence peak reduction or a poor description of the spectrum at low energies. Furthermore, a mixed-symmetry gap function (e.g., $\mathcal{R}_1+\mathcal{R}_4$) always results in a deterioration of the fit in the low-energy region. We emphasize that within the d-wave scenario, the measured ZBC is a natural consequence of the low-lying excitations and thermal smearing. Note that the experimental coherence peaks are larger than those from d-wave fits. One possible explanation for this could be a spectral weight transfer from high energies to the peaks due to strong coupling effects.[21,22]

Figure 3(b) shows the spectra taken at different temperatures with their corresponding d-wave fits. We first observe that superconductivity measured at the surface is suppressed

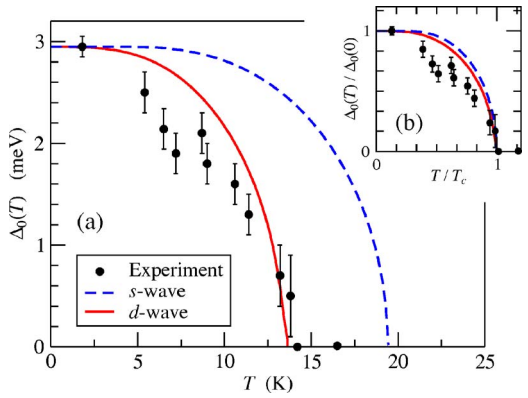

FIG. 4. (Color online) (a) Temperature dependence of the superconducting gap from the spectra in Fig. 3(b) (circles) compared to the s- and d-wave cases from solving the BCS gap equation for $\Delta_0(0)=2.95$ meV (dashed and solid curves, respectively). (b) The same data with gaps rescaled by $\Delta_0(0)$ and temperatures rescaled by the respective T_c values.

at exactly the bulk $T_c=14$ K. This confirms that our measurements probe the bulk properties of $PbMo_6S_8$. The d-wave models fit well at all temperatures, in contrast to the s wave which consistently fails to reproduce the spectral shape at low energy. The gap amplitudes $\Delta_0(T)$ from the fits to our experimental spectra are plotted as a function of temperature in Fig. 4, together with the solutions of the BCS gap equation for both the s- and d-wave symmetries. These were calculated by selecting the simplest separable coupling interaction, preserving the gap symmetry, i.e., $V_{\boldsymbol{k},\boldsymbol{k}'}=V_0\psi(\boldsymbol{k})\psi^*(\boldsymbol{k}')$, and determining V_0 so as to fix the zero-temperature gap at our experimental value (2.95 meV). The s-wave solution gives a T_c of 19.4 K, as expected from the well-known $2\Delta_0/k_BT_c$ ratio of 3.52 but clearly at variance with our experiment. On the other hand, the T_c from the 3D d-wave model is 13.6 K, giving a ratio of 5.0 in agreement with our experimental value of 4.9 ± 0.3 [Fig. 4(a)]. These results are also shown renormalized by their respective T_c values in Fig. 4(b), highlighting the facts that the presence of nodes affects the shape of the curve (and not only the $2\Delta_0/k_BT_c$ ratio) and that the experimental gap closes faster with increasing temperature than the theoretical curves.

The large low-temperature gap is also consistent with the high upper critical field: using the Fermi velocity from Ref. 23, $v_F\approx 4\times10^4$ ms^{-1}, we obtain a rough estimate of the coherence length $\xi=\hbar v_F/\pi\Delta_0\approx 28$ Å, in line with the value derived earlier from H_{c2}.[10] This very small coherence length and the large coupling ratio of 4.9 further confirm the similarity with the high-T_c materials, which has already been emphasized by Uemura *et al.*[24]

Let us now turn to the effect of the true band structure of this material. Our FLAPW (Ref. 25) calculations, in agreement with previous calculations,[1] reveal that two Mo-d bands (of width 0.7 eV) cross the Fermi level, both contributing roughly equally to the total DOS at ϵ_F. This justifies a single-band approach in calculating the superconducting properties. The normal state DOS appears constant at the energy scale of our measurements. However, the calculated Fermi surface (FS) is not spherically symmetric and exhibits significant

nesting at $\boldsymbol{Q}=0.62$ and 1.08 $(2\pi/a)$ along the [111] direction. Most strikingly, one of the two FS sheets displays two lobes above and below the basal plane. This could be of importance in the case of highly anisotropic superconducting gaps. In effect, the presence of two bands and the FS topology influence the gap distribution and could thus explain the slight disagreement for the peak heights and ZBC between the *d*-wave models and the observed spectra as well as the deviations from the calculated temperature dependence. The details of the Fermi surface could also influence the spectra through the tunneling matrix element. However, since we tunnel from a direction 54° off the main (threefold) symmetry axis, the STM tip effectively probes all relevant parts of the Fermi surface. Any further development of the model presented here would demand the knowledge of the radial dependence of the gap function, itself requiring a complete description of the pairing interaction.

In summary, we have measured the low-temperature characteristics of the quasiparticle DOS of superconducting $PbMo_6S_8$ using scanning tunneling spectroscopy. In light of these results, we conclude that a highly anisotropic gap function is the likely explanation for the low-energy excitations observed in our spectra. In particular, we have shown that our measurements are well described by 3D *d*-wave models compatible with the rhombohedral symmetry of $PbMo_6S_8$. Such *d*-wave superconductivity in $PbMo_6S_8$ could result from the very short coherence length which would favor the appearance of a repulsive component in the coupling interaction. The combination of a possible *d*-wave symmetry, a large $2\Delta_0/k_BT_c$ ratio, and a short coherence length in $PbMo_6S_8$ is strongly reminiscent of the HTS and calls for further investigation. We believe that vortex core spectroscopy, which has already revealed important differences between classical superconductors and HTS, would be the ideal tool to confirm the role played by an intrinsic short coherence length in unconventional superconductivity.

The authors particularly wish to thank M. Sigrist and F. Marsiglio for invaluable discussions. This work was supported by the Swiss National Science Foundation through the NCCR MaNEP.

*Electronic address: cedric.dubois@physics.unige.ch

[1] *Superconductivity in Ternary Compounds I*, Topics in Current Physics Vol. 32, edited by Ø. Fischer and M. B. Maple (Springer-Verlag, Berlin, 1982); *Superconductivity in Ternary Compounds*, Topics in Current Physics Vol. 34, edited by Ø. Fischer and M. B. Maple (Springer-Verlag, Berlin, 1982).

[2] F. Steglich, J. Aarts, C. D. Bredl, W. Lieke, D. Meschede, W. Franz, and H. Schäfer, Phys. Rev. Lett. **43**, 1892 (1979).

[3] H. A. Radovan, N. A. Fortune, T. P. Murphy, S. T. Hannahs, E. C. Palm, S. W. Tozer, and D. Hall, Nature (London) **425**, 51 (2003).

[4] R. J. Cava, H. Takagi, H. W. Zandbergen, J. J. Krajewski, W. F. Peck, Jr., T. Siegrist, B. Batlogg, R. B. Van Dover, R. J. Felder, K. Mizuhashi *et al.*, Nature (London) **367**, 252 (1994).

[5] Y. DeWilde, M. Iavarone, U. Welp, V. Metlushko, A. E. Koshelev, I. Aranson, G. W. Crabtree, and P. C. Canfield, Phys. Rev. Lett. **78**, 4273 (1997).

[6] D. Jérome, A. Mazaud, M. Ribault, and K. Bechgaard, J. Phys. (Paris), Lett. **41**, L95 (1980).

[7] T. Arai, K. Ichimura, K. Nomura, S. Takasaki, J. Yamada, S. Nakatsuji, and H. Anzai, Phys. Rev. B **63**, 104518 (2001).

[8] Y. Maeno, H. Hashimoto, K. Yoshida, S. Nishizaki, T. Fujita, J. G. Bednorz, and F. Lichtenberg, Nature (London) **372**, 532 (1994).

[9] M. D. Upward, L. P. Kouwenhoven, A. F. Morpurgo, N. Kikugawa, Z. Q. Mao, and Y. Maeno, Phys. Rev. B **65**, 220512(R) (2002).

[10] Ø. Fischer, Appl. Phys. **16**, 1 (1978).

[11] C. P. Poole, Jr., H. A. Farach, and R. J. Creswick, *Superconductivity* (Academic, New York, 1995).

[12] Ø. Fischer, M. Kugler, I. Maggio-Aprile, C. Berthod, and C. Renner, Rev. Mod. Phys. (to be published).

[13] C. Renner, A. D. Kent, P. Niedermann, Ø. Fischer, and F. Lévy, Phys. Rev. Lett. **67**, 1650 (1991).

[14] H. F. Hess, R. B. Robinson, and J. V. Waszczak, Phys. Rev. Lett. **64**, 2711 (1990).

[15] R. Chevrel and M. Sergent, Chap. 2 of Ref. 1.

[16] C. Dubois, P. E. Bisson, A. A. Manuel, Ø. Fischer, and S. Reymond, Rev. Sci. Instrum. **77**, 043712 (2006).

[17] U. Poppe and H. Wühl, J. Low Temp. Phys. **43**, 371 (1981).

[18] By *d* wave, we mean representations corresponding to an orbital moment of $\ell=2$ in the spherical harmonics expansion, some of which do not display a sign change.

[19] M. Sigrist and K. Ueda, Rev. Mod. Phys. **63**, 239 (1991).

[20] The residual DOS could originate from a band with a different character remaining normal (although this is not supported by our electronic structure calculations) or anomalous electronic states at the surface, for example.

[21] W. L. McMillan and J. M. Rowell, Phys. Rev. Lett. **14**, 108 (1965).

[22] J. R. Schrieffer, D. J. Scalapino, and J. W. Wilkins, Phys. Rev. Lett. **10**, 336 (1963).

[23] J. A. Woollam and S. A. Alterovitz, Phys. Rev. B **19**, 749 (1979).

[24] Y. J. Uemura, L. P. Le, G. M. Luke, B. J. Sternlieb, W. D. Wu, J. H. Brewer, T. M. Riseman, C. L. Seaman, M. B. Maple, M. Ishikawa *et al.*, Phys. Rev. Lett. **66**, 2665 (1991).

[25] P. Blaha, K. Schwarz, G. Madsen, D. Kvasnicka, and J. Luitz, *WIEN2k, An Augmented Plane Wave Plus Local Orbitals Program for Calculating Crystal Properties* (Vienna University of Technology, Austria, 2001).